Studies on the Replication of the Ring Opened Formamidopyrimidine, Fapy·dG in *Escherichia coli*†

Jennifer N. Patro,‡ Carissa J. Wiederholt,‡ Yu Lin Jiang,‡ James C. Delaney,§ John M. Essigmann,§ and Marc M. Greenberg*,‡

Department of Chemistry, Johns Hopkins University, 3400 North Charles Street, Baltimore, Maryland 21218, and Departments of Chemistry and Biological Engineering, Massachusetts Institute of Technology, Cambridge, Massachusetts 02139

Received April 2, 2007; Revised Manuscript Received June 12, 2007

ABSTRACT: Fapy·dG is produced in DNA as a result of oxidative stress from a precursor that also forms OxodG. Bypass of Fapy·dG in a shuttle vector in COS-7 cells produces G → T transversions slightly more frequently than does OxodG (Kalam, M. A., et al. (2006) *Nucleic Acids Res. 34,* 2305). The effect of Fapy·dG on replication in *Escherichia coli* was studied by transfecting M13mp7(L2) bacteriophage DNA containing the lesion within the *lacZ* gene in 4 local sequence contexts. For comparison, experiments were carried out side-by-side on OxodG. The efficiency of lesion bypass was determined relative to that of a genome containing native nucleotides. Fapy·dG was bypassed less efficiently than OxodG. Bypass efficiency of Fapy·dG and OxodG increased modestly in SOS-induced cells. Mutation frequencies at the site of the lesions in the originally transfected genomes were determined using the REAP assay (Delaney, J. C., Essigmann, J. M. (2006) *Methods Enzymol. 408,* 1). G → T transversions were the only mutations observed above background when either Fapy·dG or OxodG was bypassed. OxodG mutation frequencies ranged from 3.1% to 9.8%, whereas the G → T transversion frequencies observed upon Fapy·dG bypass were ≤1.9% in wild-type *E. coli*. In contrast to OxodG bypass, Fapy·dG mutation frequencies were unaffected by carrying out experiments in *mutM/mutY* cells. Overall, these experiments suggest that Fapy·dG is at most weakly mutagenic in *E. coli*. Steady-state kinetic experiments using the Klenow fragment of DNA polymerase I from *E. coli* suggest that a low dA misincorporation frequency opposite Fapy·dG and inefficient extension of a Fapy·dG:dA base pair work synergistically to minimize the levels of G → T transversions.

A wide variety of DNA modifications are formed when the biopolymer is exposed to oxidative conditions. In general, DNA lesions are of significant interest due to their possible genotoxic effects. Considerable attention has been paid to the effects of DNA lesions derived from 2′-deoxyguanosine, which has the most favorable oxidation potential of the native nucleotides (*1*). OxodG[1] and Fapy·dG, which form from a common intermediate, are two frequently detected lesions derived from the damage of dG (Scheme 1) (*2*). Bypass of OxodG in *Escherichia coli* and COS-7 cells gives rise to G → T transversions (*3*−*8*). Recently, Fapy·dG bypass in COS-7 cells was shown to result in G → T transversions more frequently than that of OxodG (*9*). We now report that very low frequencies of G → T transversions occur when Fapy·dG is bypassed in *E. coli* and describe the genetic effects of the lesion in several different sequence contexts.

Scheme 1: Fapy•dG and OxodG Arise from a Common Intermediate

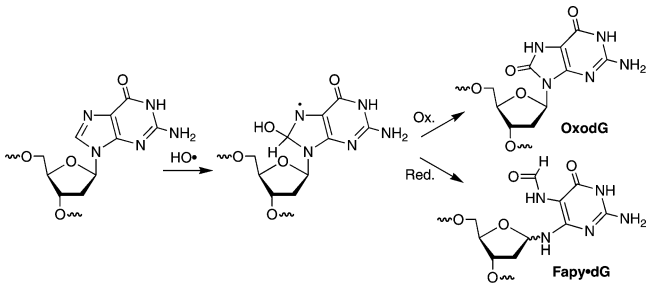

Irradiation of DNA in vitro under O_2 deficient conditions produces comparable amounts of OxodG and Fapy·dG (*10*, *11*). The ratio of OxodG to Fapy·dG increases to ∼4 under aerobic conditions, which is consistent with the involvement of O_2 in the formation of OxodG from the radical intermediate (Scheme 1). The relative amounts of Fapy·dG and OxodG detected in cells varies considerably with cell type and whether the cells are subjected to oxidative damage (*12*, *13*). For instance, Fapy·dG is present in ∼6-fold higher levels than OxodG in mouse liver cells, and is also found in relatively greater amounts in human leukemia cells exposed to ionizing radiation (*14*, *15*).

Although the incidence of a lesion is interesting, the ultimate measure of its biological importance is how it affects

† Supported by the NIH (CA-74954 to M.M.G. and CA-80024, CA-26731, and P30-ES02109 to J.M.E.).

* Author to whom correspondence should be addressed. E-mail: mgreenberg@jhu.edu.

‡ Johns Hopkins University.

§ Massachusetts Institute of Technology.

[1] Abbreviations: Fapy·dG, 2′-deoxyguanosine formamidopyrimidine; OxodG, 8-oxo-2′-deoxyguanosine; Fpg or MutM, formamidopyrimidine DNA glycosylase; MutY, 2′-deoxyadenosine mismatch repair enzyme; PAGE, polyacrylamide gel electrophoresis; REAP, restriction endonuclease and postlabeling.

10.1021/bi700628c CCC: $37.00
Published on Web 08/11/2007

replication, transcription, and whether it is capable of being repaired (*16*−*19*). Biochemical experiments suggest that Fapy·dG and OxodG interact similarly with DNA polymerase and base excision repair enzymes (*20*). For instance, Fpg selectively excises the lesions when opposite dC compared to when they are part of promutagenic base pairs with dA (*21*, *22*). In addition, dA is incised by MutY when opposite Fapy·dG, albeit considerably less efficiently than when the native nucleotide is opposite OxodG (*21*, *23*). OxodG and Fapy·dG also misdirect DNA polymerases to incorporate dA opposite them when the lesions are present in synthetic templates (*24*−*26*). Misinsertion frequencies are greater when OxodG is copied than when Fapy·dG is in the template. In addition, misincorporation of dA results from OxodG bypass even when the polymerase contains proofreading capability. Previously, translesion synthesis of templates containing Fapy·dG was examined only with a polymerase that lacked proofreading activity (Klenow exo$^-$ fragment of *E. coli* DNA Polymerase I). The experiments described herein using Klenow exo$^+$ that retains a proofreading function suggest that this property affects the outcome of replication of a single-stranded genome containing Fapy·dG in *E. coli*. Replication of vectors containing OxodG in *E. coli* consistently yield G → T transversions (*7*, *27*). Using the recently developed restriction endonuclease and postlabeling (REAP) method, Essigmann and co-workers found that OxodG gives rise to between 2.7% and 6.8% G → T transversions in wild-type *E. coli* (*5*, *6*, *28*). In this investigation, the REAP method was used to compare the replication of OxodG and Fapy·dG in *E. coli*.

EXPERIMENTAL PROCEDURES

Materials and General Methods. Oligonucleotides were prepared on an Applied Biosystems Inc. 394 DNA synthesizer. Commercially available DNA synthesis reagents, including the phosphoramidite for OxodG, were obtained from Glen Research Inc. All oligonucleotides except those containing Fapy·dG were deprotected using concentrated aqueous ammonium hydroxide as prescribed by the manufacturer's protocol. Oligonucleotides containing Fapy·dG were prepared as previously described (*29*−*31*). The oligonucleotides used are listed in Table 1. Oligonucleotides were radiolabeled with ^{32}P on the 5′-terminus by treatment with T4 polynucleotide kinase and γ-^{32}P-ATP at 37 °C for 1 h. Excess ATP and salts were removed by passing the DNA through a G-25 Sephadex (Sigma) column in TE pH 8.0. All other procedures involved standard protocols (*32*). Samples were counted on a Beckmann Coulter LS6500 scintillation counter, and gels were quantified using a Storm 840 phosphorimager and analyzed using Imagequant 5.1. DNA manipulations were carried out using standard procedures. Klenow fragment, BSA, dNTPs, *Bbs*I, *Hae*III, T4 polynucleotide kinase, and T4 DNA ligase were obtained from New England Biolabs. Inorganic pyrophosphatase and γ-^{32}P-ATP were from USB and Perkin-Elmer, respectively. T4 polynucleotide kinase for *E. coli* experiments was purchased from USB. Turbo Pfu polymerase was from Stratagene and Nuclease P1 was from Sigma-Aldrich.

Enzymatic Ligation of Fapy·dG Containing Oligonucleotides. Phosphorylation was carried out by combining T4 polynucleotide kinase (20 units) in 1 × kinase buffer (70 mM Tris-HCl (pH 7.6), 10 mM $MgCl_2$, 5 mM DTT), 1% (w/v) DTT, and γ-^{32}P-ATP (30 μCi) with 60 pmol of a 12 mer (**5**) for 1 h at 37 °C (35 μL total volume). The DNA was purified using a G-25 Sephadex column. The 14 mer scaffold (**6**, 90 pmol) and the 16 mer containing Fapy·dG (**4**, 90 pmol) were added to 5′-^{32}P-**5** in 1 × ligase buffer (50 mM Tris-HCl (pH 7.5), 10 mM $MgCl_2$, 1 mM ATP, 10 mM DTT, and 25 μg/mL BSA), heated for 5 min at 80 °C, and slowly cooled to room temperature (100 μL total volume). The sample was counted using a liquid scintillation counter, and 10 nmol of ATP and 1000 units of ligase was added to the hybridized sample and reacted for 1 h at 16 °C. The sample was partially concentrated in the Speed-vac, diluted with formamide loading buffer (100 μL) without dye, and separated on a 1.5 mm thick 20% denaturing PAGE gel. The ligated product band (**7**) was excised from the gel, eluted for 9 h in elution buffer (100 mM NaCl, 1 mM EDTA), desalted on a C18-Sep pak (Waters), and dried in the Speed-vac. The product was resuspended in 50 μL water and recounted on a liquid scintillation counter to determine the yield.

Proofreading of dA/dC Opposite dG and Fapy·dG by Klenow exo$^+$. Klenow exo$^+$ (368 nM) was reacted with 0.02 unit of pyrophosphatase for 10 min at room temperature. 5′-^{32}P-**11a**(**11b**) was hybridized to 1.5 equiv of the template (**15**, **16**) to form **19a**,**b** and **20a**,**b** by heating at 60 °C for 5 min and cooling to room temperature. Reaction mixtures containing varying concentrations of duplex (**19a** = 1−50

Table 1: Oligonucleotides Used in This Study

5′-GAA GAC CTX YGC GTC C **1a**−**d**, X = Fapy·dG **2a**−**d**, X = OxodG **3c**, X = G **a**, Y = A; **b**, Y = C; **c**, Y = G; **d**, Y = T
5′-CAA GGT GCX AAG TGG T **4**, X = Fapy·dG
5′-AGC ACG TCC CAT **5**
5′-ACG TGC TAC CAC TT **6**
5′-CAA GGT GCX AAG TGG TAG CAC GTC CCA T **7**, X = Fapy·dG **8**, X = G
5′-GGT CTT CCA CTG AAT CAT GGT CAT AGC **9**
5′-AAA ACG ACG GCC AGT GAA TTG GAC GC **10**
5′-ACC ATG GGA CGT GCT GTY **11a**, Y = C **11b**, Y = A
5′-ACC ATG GGA CGT GCT GA **12**
5′-ATG GGA CGT GCT ACC AC **13**
5′-ATG GGA CGT GCT ACC ACT T **14a**, Y = C **14b**, Y = A
5′-AGG CGT TCA ACG TGC AGT XAC AGC ACG TCC CATGGT **15**, X = Fapy·dG **16**, X = dG
5′-AGG CGT TCA ACG TGC AGT XTC AGC ACG TCC CATGGT **17**, X = Fapy·dG **18**, X = G

nM, **19b** = 1−30 nM, **20a** = 3−15 nM, **20b** = 3−25 nM) were prepared by mixing DNA (5 μL) with a 2 × enzyme solution (5 μL) containing Klenow (1.472 nM) in 20 mM Tris-HCl (pH 7.5), 10 mM $MgCl_2$, 15 mM DTT. Reactions were run for 30 min (**19a**), 6 min (**19b**), 12 min (**20a**), or 20 min (**20b**) and then quenched with 95% formamide loading buffer (20 μL). Samples were denatured for 1 min at 90 °C, cooled on ice, and separated on a 20% denaturing PAGE gel. Kinetic parameters reported represent the average of three separate experiments each carried out in triplicate.

Standing Start Synthesis Opposite dG/Fapy·dG by Klenow exo$^+$ and exo$^-$. Klenow exo$^+$ or exo$^-$ was reacted with pyrophosphatase as described above. 5′-^{32}P-**12** was hybridized to 1.5 equiv of the template (**17**, **18**) to form **21** and **22** by heating at 60 °C for 5 min and cooling to room temperature. Duplex DNA (**21**, **22**, 20 nM) was mixed with varying concentrations of dCTP (**21** = 1−100 nM, **22** = 1−500 nM) or dATP (**21** = 10−500 μM, **22** = 1−50 μM). Klenow exo$^+$/exo$^-$ (1 nM) in 2 × reaction buffer (20 mM Tris-HCl (pH 7.5), 10 mM $MgCl_2$, 15 mM DTT) was added (5 μL) to the dNTP/DNA mixture (5 μL). Reactions were run at room temperature (20 min for dCTP and 15 min for dATP) and quenched with 95% formamide loading buffer. Samples were denatured for 1 min at 90 °C and loaded onto a 20% denaturing polyacrylamide gel.

Velocities were calculated by using the equation $[100I_1/(I_0 + 0.5I_1)]t$ where t is the time of the reaction, I_1 is the amount of product formed (18 mer), I_0 is the amount of starting material, and I_1 is less than 25% of I_0 (*33*, *34*). Each reaction was carried out in triplicate, and the V_{max} and K_M were determined by a nonlinear curve fit.

Running Start Kinetics of Translesional Synthesis of Fapy·dG by Klenow exo$^+$. Klenow exo$^+$ was treated with pyrophosphatase as described above. The primer (5′-^{32}P-**13**) and template (**7**) were annealed together at 200 nM to produce **23** by heating at 90 °C and cooling to room temperature. Klenow exo$^+$ was diluted to 25.7 nM in 5 × reaction buffer (50 mM Tris-HCl (pH 7.5), 25 mM $MgCl_2$, 37.5 mM DTT, and 0.5 mg/mL BSA). The enzyme was added to **23** to make a 2 × enzyme/DNA cocktail (final DNA concentration = 100 nM; enzyme = 10 nM). This 2 × solution was incubated for 1 min at room temperature and then added (5 μL) to a 2 × dNTP solution (5 μL) containing running start and rescue nucleotides (dTTP and dGTP, respectively, 10 μM) and substrate dNTP (dCTP (20−600 nM) or dATP (2−20 μM)). The reactions were run for 8 min (dCTP) or 12 min (dATP) at room temperature, quenched with 95% formamide/1 mM EDTA, denatured by heating for 1 min at 90 °C and placed on ice. The reactions were loaded on a 20% denaturing PAGE gel and electrophoresed at 25 mA for 3.5 h. Relative velocities were calculated by taking the ratio of translesional synthesis product plus extension product versus the insertion of the products resulting from incorporation of running start nucleotides $[(I_{t+1} + I_t)/(I_{t-1} + I_{t-2})]$, where I_t and I_{t+1} are the amounts of translesional incorporation and extended products, respectively. I_{t-1} and I_{t-2} correspond to the amounts of products due to incorporation of running start nucleotides prior to reaching the lesion. The ratio was plotted versus substrate concentration, and a K_M and relative V_{max} of translesion incorporation were calculated. The insertion of dC opposite Fapy·dG was fitted using nonlinear regression analysis, while the insertion of dA opposite Fapy·dG could not be saturated so the data was fit linearly (*33*, *34*). The $(V_{max}/K_M)_{rel}$ was determined from the average of three separate experiments each carried out in triplicate.

Kinetics of Extension Past dG:dC, dG:dA, and Fapy·dG:dC. Primers (5′-^{32}P-**14a**, -**14b**) and templates (**7**, **8**, 320 nM) were hybridized by heating for 5 min at 90 °C and cooling to room temperature. Klenow exo$^+$ was treated with pyrophosphatase as described above. A 4 × enzyme solution (4 nM) containing 0.4 mg/mL BSA and 4 × reaction buffer (40 mM Tris-HCl (pH 7.5), 20 mM $MgCl_2$, and 30 mM DTT) was added to varying concentrations of dGTP (**24a**, 1−30 nM; **24b**, 0.1−1 mM; **25a**, 0.1−2.5 μM, and a final concentration of **24** or **25** of 80 nM). The reaction was run at 25 °C for 3 min (**24a**), 15 min (**24b**), or 7 min (**25a**), quenched with 95% formamide loading buffer, and placed on ice. The samples were denatured for 1 min at 90 °C and put back on ice, after which they were separated by 20% denaturing PAGE. The amount of extended primer (I_{t+1}) divided by the amount of primer excised (I_{t-1}) was quantitated. The ratio (I_{t+1}/I_{t-1}) was plotted versus the substrate concentration and fit via nonlinear regression analysis. The K_M was determined in the same manner as other standard kinetic reactions, but instead of calculating a V_{max}, a ratio of extension versus excision was determined as k_{pol}/k_{exo} (*33*, *34*).

M13 Genome Construction and Replication in E. coli. Each insert (**1**−**3**) was cloned into the M13mp7(L2) vector in triplicate as previously described (*35*, *36*). Briefly, the insert (10 pmol) was phosphorylated and ligated into 6 pmol of *Eco*RI-digested M13mp7(L2) using complementary scaffolds. After digestion of the scaffolds with T4 DNA polymerase, the vectors were purified by phenol extraction and Centricon 100 membrane filtration. The recovery was quantitated by UV ($\epsilon_{260} = 7.152 \times 10^7$ L/mol·cm). For SOS-induction, AB1157 cells were grown to an OD_{600} of 0.3, pelleted, and resuspended in 10 mM $MgSO_4$. The cells were irradiated with 254 nm light at 45 J/m^2, added to 50 mL of 2xYT media, and incubated at 37 °C for 40 min (*32*). SOS-induced and noninduced AB1157 cells were pelleted, washed with ice-cold water, and finally resuspended in 10% glycerol. Competent AB1157 cells (100 μL) were electroporated with 1 pmol of the vector (∼2.64 kV, 4.74 ms), and a portion was immediately plated with X-Gal and IPTG to assess lesion bypass, by comparing the number of blue transformants from the vector containing the lesion of interest to the number of transformants of a control vector containing dG at the appropriate position.

REAP Assay To Determine Mutation Frequency. Mutation analysis was carried out using the restriction endonuclease and postlabeling (REAP) assay which has previously been described (*35*, *36*). Briefly, viral DNA was recovered from the growth medium and PCR amplified. Following digestion with *Bbs*I and shrimp alkaline phosphatase, the DNA was ^{32}P-labeled and further digested with *Hae*III. The desired 18 mer product was purified using 20% denaturing PAGE and desalted using a G25 Sephadex column. Finally, the samples were digested with nuclease P1 and nucleotides separated on a PEI cellulose TLC plate which was run with saturated $(NH_4)_2HPO_4$ and H_3PO_4, pH 5.8.

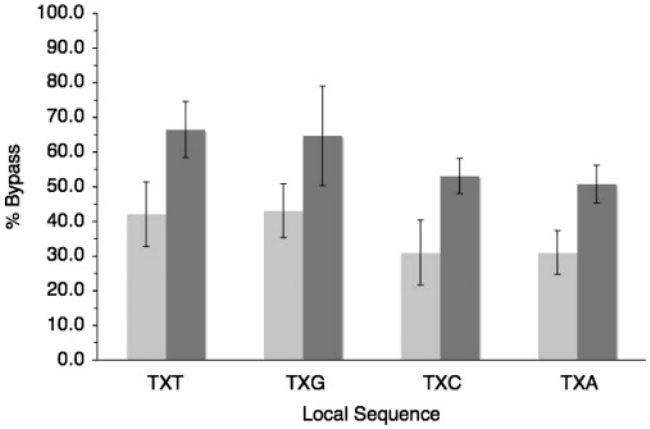

FIGURE 1: Percent bypass of Fapy·dG (**1a**−**d**, light gray) and OxodG (**2a**−**d**, dark gray) in wild-type *E. coli* as a function of flanking sequence.

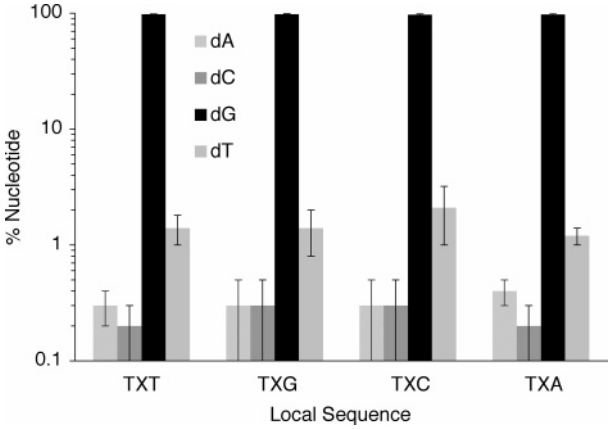

FIGURE 2: Percent nucleotide incorporation in place of Fapy·dG (**1a**−**d**) as a function of flanking sequence following replication in wild-type *E. coli*. X = Fapy·dG.

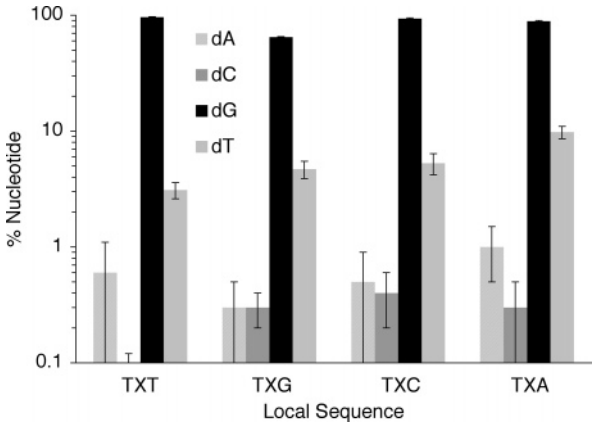

FIGURE 3: Percent nucleotide incorporation in place of OxodG (**2a**−**d**) as a function of flanking sequence following replication in wild-type *E. coli*. X = OxodG.

RESULTS

Fapy·dG Bypass Efficiency in E. coli. Single-stranded vectors containing dG, OxodG, or Fapy·dG flanked by dT on the 5′-side and dA, dC, dG, or dT on the 3′-side were prepared from *Eco*RI linearized M13mp7(L2) vectors. The oligonucleotide inserts were incorporated within the *lacZ* gene, enabling one to detect replication through the insert by measuring the number of blue plaques. The percent bypass for OxodG or Fapy·dG was determined by comparing the number of blue plaques obtained upon transfection with a plasmid containing the appropriate lesion to those obtained from a plasmid containing dG (Figure 1). Fapy·dG bypass ranged from 31 ± 6% to 43 ± 9% depending upon the identity of the 3′-adjacent nucleotide. The bypass efficiency of OxodG (51−66%) was consistently higher than that of Fapy·dG in otherwise identical sequences. Because bypass is slowed when the Fapy·dG is present, we investigated whether replication is aided by the SOS polymerases (Pol II, Pol IV, or Pol V), whose production is upregulated when cells are exposed to UV irradiation. When SOS-induced cells were transfected with Fapy·dG (**1c**), the average bypass efficiency increased to 59% but there was a large variation (38%) resulting in no statistically significant change. OxodG (**2c**) bypass efficiency increased to a level commensurate with that of the native nucleotide.

Nucleotide Incorporation Opposite Fapy•dG in E. coli Using the REAP Assay. The mutation frequencies of Fapy·dG were determined in *E. coli* in 4 sequence contexts (Figure 2). For comparison, the mutation frequencies of the biochemically related, and well-studied OxodG (Figure 3) in the same sequence contexts, as well as dG were determined in side-by-side experiments. The data presented are an average of at least two experiments for Fapy·dG and OxodG, in which each experiment consisted of 3 replicates. The levels of dA and dC present in the progeny produced upon replication of plasmid containing Fapy·dG were statistically indistinguishable from the levels detected in the REAP analysis of plasmid containing dG. The levels of dT measured in the REAP assays of Fapy·dG (Table 2) and OxodG (Table 3) replication resulting from dA misincorporation were consistently greater than those obtained from dG. Consistent with previous reports, OxodG gave rise to 3.1−9.8% G → T transversions in wild-type cells. When flanked by a 3′-dA, OxodG had a mutation frequency that was ∼2-fold higher than in any of the other sequences studied. The mutation frequencies obtained upon OxodG replication were consistently higher than those detected from the respective sequences containing Fapy·dG. Replication of Fapy·dG in

Table 2: G → T Transversions Resulting from Fapy·dG Replication[a]

sequence (5′→3′)	% dG → dT transversions	*P* value[b]
T-Fapy·dG-T	1.3 ± 0.6	0.021
T-Fapy·dG-G	1.3 ± 0.7	0.012
T-Fapy·dG-C	1.9 ± 1.2	0.008
T-Fapy·dG-A	1.2 ± 0.3	0.002
T-G-G	0.6 ± 0.2	n/a

[a] Values are the averages (±std dev) of at least 2 independent experiments each run in triplicate. [b] Determined using a Mann−Whitney test.

Table 3: G → T Transversions Resulting from OxodG Replication[a]

sequence (5′→3′)	% dG → dT transversions	*P* value[b]
T-OxodG-T	3.1 ± 1.1	0.004
T-OxodG-G	4.8 ± 0.8	0.004
T-OxodG-C	5.3 ± 1.9	0.004
T-OxodG-A	9.8 ± 1.6	0.004
T-G-G	0.5 ± 0.2	n/a

[a] Values are the averages (±std dev) of 2 independent experiments run in triplicate. [b] Determined using a Mann−Whitney test.

Table 4: G → T Transversions Resulting from Replication of Fapy·dG and OxodG in *mutM/mutY* Cells[a]

sequence (5′→3′)	% G → T transversions
T-Fapy·dG-T	1.6 ± 0.5
T-Fapy·dG-G	1.2 ± 0.2
T-Fapy·dG-C	2.1 ± 0.4
T-Fapy·dG-A	0.7 ± 0.3
T-OxodG-G	37.6 ± 3.5

[a] Values are the average (±std dev) of 1 experiment run in triplicate.

wild-type *E. coli* gave levels of dT that ranged from only 1.2% to 1.9% depending on the sequence context. Because the mutation frequencies of Fapy·dG were so low and bordered on the detection limit of the REAP assay, we applied a nonparametric Mann−Whitney test to verify that they were statistically distinguishable from the levels detected in plasmids produced from dG replication (Table 2). In all sequence contexts, the higher mutation frequencies of both Fapy·dG and OxodG than the background observed from dG bypass were statistically significant. In addition, the different levels of G → T transversions obtained when OxodG was bypassed in various sequences were significantly different ($P < 0.025$) from the other sequence contexts tested with the exception of the T-OxodG-G compared to T-OxodG-C sequence (data not shown). However, the mutation frequency of Fapy·dG did not significantly vary among sequences.

Differences in the replication of plasmids containing Fapy·dG *mutM/mutY* and OxodG were also evident when the corresponding plasmids were transfected into cells lacking the Fpg and MutY repair proteins (Table 4). OxodG bypass resulted in a nearly 8-fold increase in G → T transversions. However, replication of Fapy·dG was unaffected. Finally, the percent of G → T transversions in SOS-induced wild-type cells produced following transfection of plasmid containing the T-Fapy·dG−dG (**1c**) sequence (0.3%) was statistically indistinguishable from the level of thymidine found in the progeny produced from replication of an identical plasmid containing dG (**3c**). While the level of G → T transversions resulting from bypass of the respective OxodG (**2c**) lesion was above background (6.6%), it was not significantly different from the mutation frequency observed in non-SOS-induced wild-type cells.

Steady-State Kinetic Analysis of Proofreading by Klenow exo$^+$. The effect of exonucleolytic excision on nucleotide misinsertion was probed directly by determining the steady-state kinetic parameters for the removal of dA (**20b**) and dC (**20a**) opposite Fapy·dG (Table 5). For comparison, excision of dA (**19b**) and dC (**19a**) opposite dG was also carried out. These experiments indicate that, when opposite dG, dA is excised by Klenow exo$^+$ ~3-fold more efficiently than is dC. However, when the template contains Fapy·dG, dC and dA are excised with comparable efficiencies that are on par with that of a dG:dA mispair. With the exception of the Fapy·dG:dC base pair, differences in K_M are mostly responsible for the variation in the specificity constant. The negligible difference in Klenow exo$^+$ excision efficiencies between Fapy·dG:dA and Fapy·dG:dC base pairs contrasts with those determined for OxodG opposite the respective native nucleotides, where excision is several-fold higher when the lesion is in a promutagenic base pair (*37*).

Table 5: Steady-State Kinetic Parameters for the Excision of dA and dC Opposite dG and Fapy·dG[a,b]

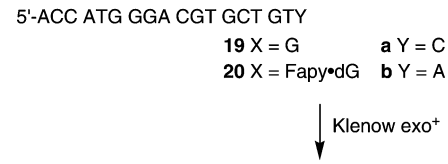

template:primer base pair	k_{cat} (min^{-1})	K_M (nM)	k_{cat}/K_M (min^{-1}·nM^{-1})
dG:dC **(19a)**	$7.1 \pm 0.8 \times 10^{-2}$	14.3 ± 1.6	$5.0 \pm 0.7 \times 10^{-3}$
dG:dA **(19b)**	$9.2 \pm 1.9 \times 10^{-2}$	6.5 ± 1.9	$1.5 \pm 0.3 \times 10^{-2}$
Fapy•dG:dC **(20a)**	$3.4 \pm 1.3 \times 10^{-2}$	2.5 ± 1.0	$1.4 \pm 0.3 \times 10^{-2}$
Fapy•dG:dA **(20b)**	$7.1 \pm 1.7 \times 10^{-2}$	3.9 ± 0.6	$1.8 \pm 0.2 \times 10^{-2}$

[a] Reactions carried out at 298 K. [b] Kinetic values presented are the average of at least 3 experiments. Each experiment consists of 3 replicates.

Steady-State Kinetic Analysis of Translesional Synthesis by Klenow Fragment. Incorporation of dC and dA opposite Fapy·dG and dG were examined under standing start and running start conditions (*33*, *34*). In running start experiments the lesion is positioned 3 or more nucleotides downstream from the 3′-end of the primer. In a standing start experiment the first nucleotide to be incorporated is opposite the lesion. Standing start measurements were made using Klenow exo$^-$ (Table 6) and Klenow exo$^+$ (Table 7). Only the latter form of the Klenow fragment was employed in running start experiments. Standing start experiments were carried out using primer−template complexes **21** and **22**. These duplexes differ from those used previously in that the 3′-adjacent flanking nucleotide is dT instead of dA (*26*). Klenow exo$^-$ exhibited comparable misinsertion frequency (F_{ins}) of dA opposite dG in **21** as it did when the 3′-adjacent nucleotide was dA. However, the F_{ins} of dA opposite Fapy·dG decreased almost 60-fold when the downstream flanking nucleotide in the template was changed from dA to dT (**22**). The decrease is due mostly to a reduction in the efficiency with which dA is incorporated opposite Fapy·dG (~15-fold) and only modestly by an increase in the V_{max}/K_M for translesional incorporation of dC (<4-fold). Even in this less mutagenic sequence, Klenow exo$^-$ misincorporates dA opposite the lesion ~20-fold more frequently than when the native nucleotide is present in the template.

Translesional synthesis in **21** and **22** by Klenow exo$^+$ differed slightly from experiments carried out using enzyme that lacked proofreading activity (Table 7). Comparing V_{max}/K_M for dC and dA incorporation opposite dG indicates that the fidelity of Klenow exo$^+$ was ~7-times greater than Klenow exo$^-$. The decreased F_{ins} for dA opposite dG was attributed mostly to a decrease in V_{max}/K_M translesion incorporation of dA. In contrast, the misinsertion frequency for dA incorporation opposite Fapy·dG increased ~3.5-fold when Klenow exo$^+$ replaced Klenow exo$^-$. Thus, Fapy·dG has a misinsertion frequency that is ~500-fold higher than dG, even when the polymerase has proofreading activity. However, the increased F_{ins} was due entirely to a decrease in the V_{max}/K_M for dC incorporation opposite the lesion. The misinsertion frequency for dA opposite Fapy·dG in **22** is

Table 6: Steady-State Kinetic Parameters for Nucleotide Incorporation Opposite dG and Fapy·dG by Klenow Exo$^-$ under Standing Start Conditions[a,b]

3'-TGG TAC CCT GCA CGA CTX TGA CGT GCA ACT TGC GGA
5'-ACC ATG GGA CGT GCT GA

21 X = G **22** X = Fapy•dG

↓ Klenow exo$^-$ dNTP

3'-TGG TAC CCT GCA CGA CTX TGA CGT GCA ACT TGC GGA
5'-ACC ATG GGA CGT GCT GAN

X	dNTP	K_M (μM)	V_{max} (%·min^{-1})	V_{max}/K_M (%·min^{-1}·M^{-1})	F_{ins}[c]
dG (**21**)	C	$4.6 \pm 2.4 \times 10^{-3}$	1.6 ± 0.8	$3.5 \pm 2.5 \times 10^{8}$	1.0
dG (**21**)	A	54.2 ± 23.2	0.8 ± 0.3	$1.5 \pm 0.9 \times 10^{4}$	4.3×10^{-5}
Fapy·dG (**22**)	C	$5.6 \pm 1.8 \times 10^{-2}$	4.2 ± 0.5	$7.5 \pm 2.6 \times 10^{7}$	1.0
Fapy·dG (**22**)	A	49.3 ± 6.5	3.0 ± 0.9	$6.1 \pm 2.0 \times 10^{4}$	8.1×10^{-4}

[a] Reactions carried out at 298 K. [b] Kinetic values presented are the average of at least 3 experiments. Each experiment consists of 3 replicates. [c] F_{ins} = (V_{max}/K_M, X = dG or Fapy·dG, dNTP = A; "incorrect")/(V_{max}/K_M, X = dG or Fapy·dG, dNTP = C; "correct").

Table 7: Steady-State Kinetic Parameters for Nucleotide Incorporation Opposite dG and Fapy·dG by Klenow Exo$^+$ under Standing Start Conditions[a,b]

3'-TGG TAC CCT GCA CGA CTX TGA CGT GCA ACT TGC GGA
5'-ACC ATG GGA CGT GCT GA

21 X = G **22** X = Fapy•dG

↓ Klenow exo$^+$ dNTP

3'-TGG TAC CCT GCA CGA CTX TGA CGT GCA ACT TGC GGA
5'-ACC ATG GGA CGT GCT GAN

X	dNTP	K_M (μM)	V_{max} (%·min^{-1})	V_{max}/K_M (%·min^{-1}·M^{-1})	F_{ins}[c]
dG (**21**)	C	$1.0 \pm 0.3 \times 10^{-3}$	$4.7 \pm 1.3 \times 10^{-1}$	$4.7 \pm 0.1 \times 10^{8}$	1.0
dG (**21**)	A	52.0 ± 34.0	$1.1 \pm 0.1 \times 10^{-1}$	$2.8 \pm 1.7 \times 10^{3}$	6.0×10^{-6}
Fapy·dG (**22**)	C	$4.5 \pm 1.4 \times 10^{-2}$	1.0 ± 0.3	$2.1 \pm 0.1 \times 10^{7}$	1.0
Fapy·dG (**22**)	A	8.5 ± 0.2	5.0 ± 0.7	$5.9 \pm 0.9 \times 10^{4}$	2.8×10^{-3}

[a] Reactions carried out at 298 K. [b] Kinetic values presented are the average of at least 3 experiments. Each experiment consists of 3 replicates. [c] F_{ins} = (V_{max}/K_M, X = dG or Fapy·dG, dNTP = A; "incorrect")/(V_{max}/K_M, X = dG or Fapy·dG, dNTP = C; "correct").

still only <1%, which in contrast, is an order of magnitude lower than its F_{ins} when the lesion is flanked on its 5′-side by dA (*26*).

3'-TAC CCT GCA CGA TGG TGA AXC GTG GAA C
5'-ATG GGA CGT GCT ACC AC

23 X = Fapy•dG

Carrying out translesional synthesis using a running start provides more insight into the competition between polymerization and proofreading than does a standing start experiment (*33*, *34*). Duplex **23** was used in running start experiments. Thymidine triphosphate and dGTP were used as the running start and rescue nucleotide triphosphates, respectively. These nucleotides were present at saturating concentrations, but control experiments showed that neither dTTP nor dGTP was incorporated opposite Fapy·dG under these conditions (data not shown). The incorporation velocity of dC opposite Fapy·dG ($V_{max(rel)} = 1.9 \pm 1.0$, $K_M = 99.0 \pm 59.0$ nM, $(V_{max}/K_M)_{rel} = 2.2 \pm 0.9 \times 10^7$) under running start conditions exhibited a nonlinear dependence upon triphosphate concentration as expected for a process under Michaelis−Menten conditions, and were the average of 7 experiments, each carried out in triplicate (see Figure 4A for the results of a representative experiment). In contrast, the velocity of dA incorporation opposite Fapy·dG varied linearly with respect to dATP concentration (see Figure 4B for the results of a representative experiment). The $(V_{max}/K_M)_{rel}$ of $3.2 \pm 0.5 \times 10^4$ was obtained as the average of 3 experiments by determining the slope of the linear dependence of velocity on dATP concentration. The F_{ins} (1.5×10^{-3}) obtained by determining the ratio of the average $(V_{max}/K_M)_{rel}$ for dA versus dC incorporation from the running start method is comparable to that determined under standing start conditions (Table 7). This linear dependence is consistent with a situation in which translesion synthesis is very slow and/or proofreading is significantly increased compared to when a cognate nucleotide is incorporated (*33*, *34*).

Steady-State Kinetic Analysis of Extension Past Fapy·dG by Klenow Fragment. Previous experiments using Klenow exo$^-$ indicated that extension past a Fapy·dG:dC(dA) base pair was ~100-fold slower than a dG:dC base pair (*26*). The ratio of the efficiency for the polymerase to extend past the base pair versus its exonuclease activity (k_{pol}/k_{exo}) was determined using duplexes **24a**,**b** and **25a**,**b** by measuring

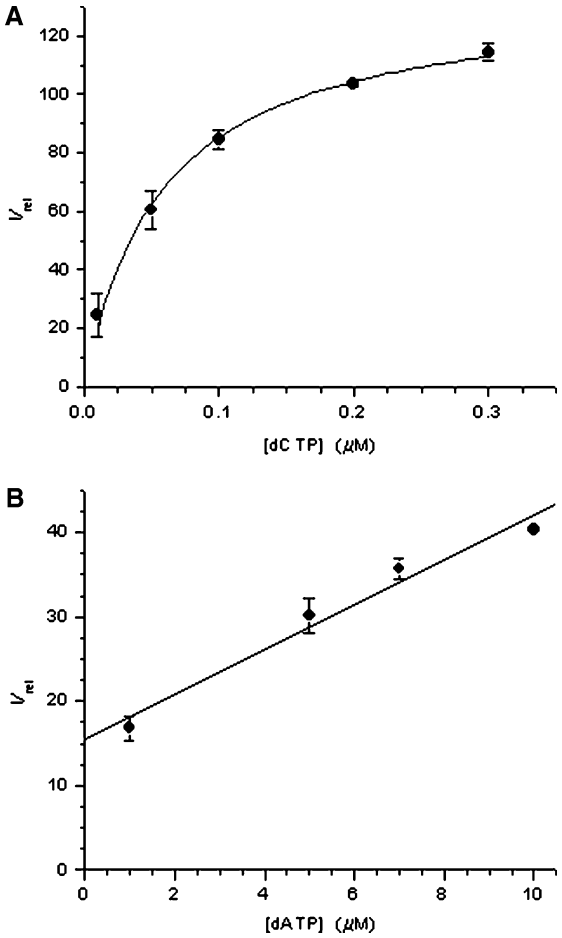

FIGURE 4: Running start kinetics describing nucleotide incorporation opposite Fapy·dG in **23** by Klenow exo$^+$. Incorporation of dCTP (A) or dATP (B) opposite Fapy·dG.

the ratio of extended product versus excised product as a function of nucleotide triphosphate concentration (*33*, *34*). For comparison, k_{pol}/k_{exo} was determined for dG:dC and dG:dA base pairs (Table 8). As expected, the primer in the duplex containing the correct base pair (**24a**) is extended much more rapidly than it undergoes excision, whereas k_{pol}/k_{exo} is much less than 1 for the dG:dA containing duplex (**24b**). Although extension of a Fapy·dG:dC base pair is 3 times more efficient than excision (Figure 5, Table 8), the ratio of these rate constants is much smaller than in a duplex containing a dG:dC base pair. Finally, extension of dA opposite Fapy·dG (**25b**) was not observed at concentrations of dGTP (the next nucleotide to be incorporated) as high as 2.5 μM, indicating that excision is far more efficient than extension.

DISCUSSION

Formamidopyrimidines are common DNA lesions. *N*-Alkylated forms result from mild alkaline hydrolysis of *N*7-alkylated purines (*38*−*40*). The simplest of these that is derived from 2′-deoxyguanosine, *N*7-Me-Fapy·dG, is a potent block of DNA polymerase (*41*). The respective unsubstituted formamidopyrimidine lesion, Fapy·dG, is formed from the most readily oxidized native nucleotide via a common intermediate from which OxodG is also produced. Although the two lesions are formed in comparable amounts, Fapy·dG is less well studied (*20*). This situation has been changing over the past 5 years, since chemical methods for the synthesis of oligonucleotides containing Fapy·dG have been reported (*29*−*31*).

Table 8: Steady-State Kinetic Analysis for Nucleotide Extension Past dG and Fapy·dG Relative to Excision by Klenow Exo$^+$ under Standing Start Conditions[a]

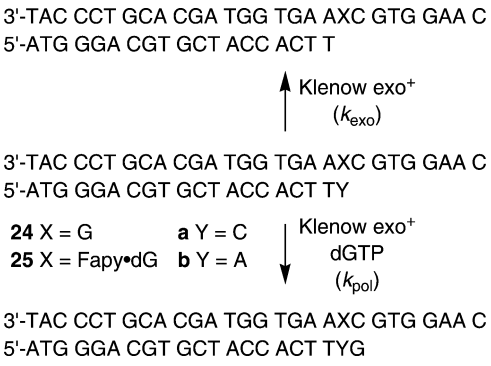

X	Y	k_{pol}/k_{exo}
dG (**24a**)	C	60
dG (**24b**)	A	0.1
Fapy·dG (**25a**)	C	3.0 ± 0.3[b]
Fapy·dG (**25b**)	A	

[a] Reactions carried out at 298 K. [b] Kinetic values presented are the average of at least 3 experiments. Each experiment consists of 3 replicates.

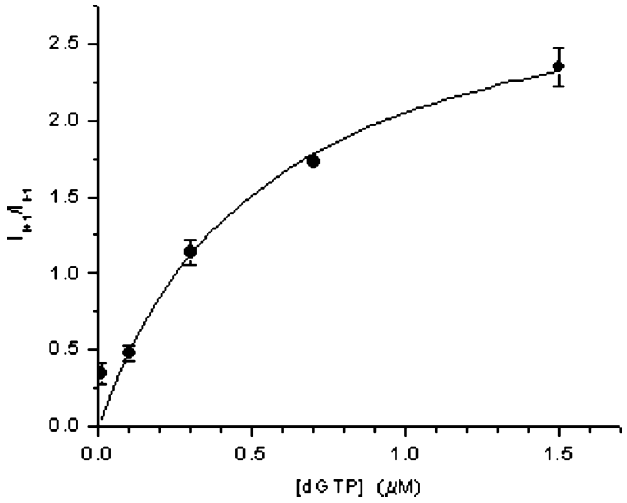

FIGURE 5: Determination of efficiency of extension versus excision in **25a** by Klenow exo$^+$.

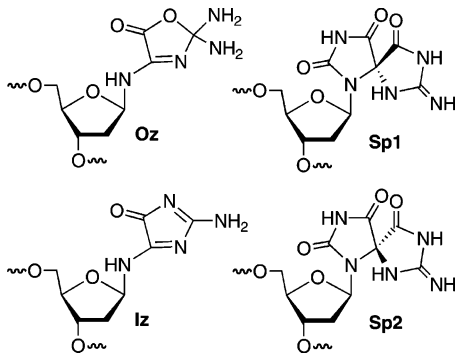

Access to chemically synthesized oligonucleotides containing Fapy·dG enabled us to construct single stranded

genomes that were used to transfect *E. coli*. Experiments were carried out alongside genomes containing dG and OxodG in order to calibrate the observations made regarding Fapy·dG. Fapy·dG was bypassed less efficiently in *E. coli* than was the native nucleotide and OxodG in all 4 sequence contexts examined (Figure 1). The bypass efficiency of Fapy·dG was comparable to those of other monocyclic guanine lesions such as oxazalone (Oz) and aminoimidazalone (Iz).-(*6*, *42*) In contrast, Fapy·dG bypass was significantly greater than the Sp1 and Sp2 spirocyclic dihydantoins (derived from OxodG oxidation) and abasic lesions (*5*, *28*, *43*). We posit that the qualitative differences and similarities in bypass levels are a reflection of the structures of the lesions. Fapy·dG, Oz, and Iz share a common more conformationally mobile structural motif in which the glycosidic nitrogen is no longer part of a ring but serves as the covalent link to the remaining cyclic component. In addition to greater conformational flexibility compared to dG or OxodG, the acyclic glycosidic nitrogen in Fapy·dG, Oz, and Iz facilitates α,*β*-configurational isomerization, because the nitrogen lone pair is no longer part of the aromatic ring system, and is therefore free to participate in a transient iminium bond with the glycosidic carbon. Indeed, facile epimerization is observed in the formamidopyrimidines (*44*, *45*). These conformational and configurational stereochemical effects may be responsible for the greater difficulty that DNA polymerase(s) experiences when bypassing these lesions. The spirocyclic lesions (Sp1, Sp2) and abasic sites may be even more difficult to bypass due to their distorted structures and complete absence of a nucleobase, respectively (*5*, *28*, *43*). The relatively modest distortion present in OxodG and Fapy·dG, as well as the monocyclic lesions (Oz, Iz), is also consistent with the absence of a significant effect of SOS-induction on bypass efficiency. In contrast, bypass of Sp1, Sp2, and abasic lesions increases considerably when error-prone polymerase production is upregulated following SOS-induction (*5*, *43*).

The fact that Fapy·dG replication in wild-type *E. coli* does not require bypass polymerases is an important consideration when explaining the observed mutational frequencies (≤1.9% G → T transversions). The mutation frequencies detected from Fapy·dG are significantly lower than any of the aforementioned lesions derived from dG, but statistically distinguishable from dG background levels. Comparing the structure of Fapy·dG to other dG derived lesions enables us to speculate why Fapy·dG gives rise to such low G → T transversion frequencies. The extremely high mutation frequencies of Oz, Iz, and the spirodihydantoins (Sp1, Sp2) can be rationalized based upon their hydrogen-bonding patterns that are distinct from dG (*5*, *6*, *28*, *42*). In contrast, OxodG and Fapy·dG, which exhibit lower mutation frequencies than Oz, Iz, Sp1, or Sp2, share a common structural feature. When OxodG and Fapy·dG are in the *anti*-conformation, they present a hydrogen-bonding pattern to a polymerase that is identical to that of dG. Although the *anti*-conformation lesions can form two hydrogen bonds when base paired with dA, this is disfavored for steric reasons. One explanation for why Fapy·dG is less mutagenic in *E. coli* than OxodG could be that it is less prone to adopt the *syn*-conformation in which thymine-like hydrogen-bonding patterns are presented to the polymerase (Scheme 2). While steric interactions between the C8-substituent in OxodG and the deoxyribose destabilize the *anti*-conformational isomer, the rotational freedom of Fapy·dG may enable the formamide group to adopt a conformation in which the respective steric interactions between the carbonyl oxygen and deoxyribose are alleviated (*46*−*49*). This explanation is consistent with kinetic studies using the Klenow fragment of DNA polymerase I, which show that translesion incorporation of dA is considerably less efficient opposite Fapy·dG (Table 6, 7) than OxodG (*24*−*26*).

Scheme 2: Fapy•dG and OxodG Can Base Pair with dA When in the *syn*-Conformation

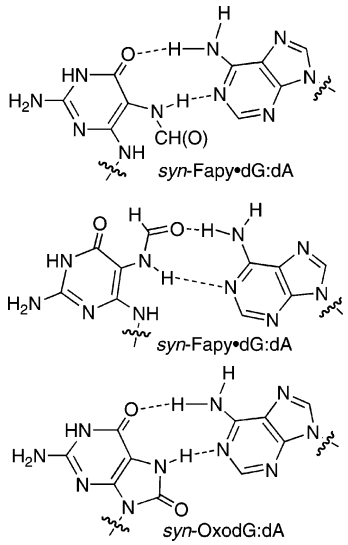

The Klenow fragment is often used as a model enzyme to study replication in *E. coli*. Steady-state kinetic experiments were used to illuminate the contributions of various steps of Fapy·dG bypass toward the low mutation frequencies we observed in *E. coli*. Measuring proofreading directly using duplexes in which a 3′-terminal dC or dA is opposite dG or Fapy·dG indicated that either nucleotide opposite the lesion is excised more rapidly than dC opposite dG (Table 5). However, the excision rate is only 3-fold greater than when dC is opposite dG (Table 5), suggesting that proofreading plays a minor role in maintaining genomic integrity when Fapy·dG was bypassed. Nucleotide incorporation kinetic experiments on Fapy·dG containing templates substantiated this proposal. Standing start translesional synthesis experiments using Klenow exo$^-$ (Table 6) and Klenow exo$^+$ (Table 7) resulted in similar dA misincorporation frequencies (F_{ins}). F_{ins} would have been much greater when using Klenow exo$^-$ if proofreading played a major role in Fapy·dG bypass. Furthermore, the similarity when F_{ins} was measured in standing start (Table 7) and running start experiments (Table 8) also indicated that Klenow exo$^+$'s exonuclease activity had little effect on Fapy·dG replication. We would have observed a lower F_{ins} when using Klenow exo$^+$ if proofreading played a large role in nucleotide incorporation opposite Fapy·dG.

The modest increase of proofreading compared to a native nucleotide not withstanding, the F_{ins} of dA by Klenow exo$^-$, which was as high as 4.8%, suggests that there must be another step that mitigates replication errors opposite Fapy·dG in *E. coli* (*26*). Steady-state kinetic experiments (Table 8) indicate that slow extension past Fapy·dG:dA base pairs protects against mutations. Comparing the ratio of extension

relative to excision (k_{pol}/k_{exo}) of a duplex containing dC opposite Fapy·dG (**25a**) to that of a native base pair (**24a**) shows that extension past the lesion is inhibited significantly. These data are qualitatively consistent with those reported previously using Klenow exo$^-$ (*26*). Moreover, extension past a Fapy·dG:dA base pair (**25b**) is so difficult that excision is able to compete. Extension is not observed, and k_{pol}/k_{exo} cannot be measured. It should be noted that extension of OxodG:dA base pairs is sufficiently rapid that no evidence for excision is observed in the presence of the appropriate dNTPs (*24*). These kinetic data suggest that mutation frequencies observed upon Fapy·dG bypass are considerably lower than those of OxodG because of an inherently lower F_{ins} of dA and subsequent slow extension, which enables the polymerase's exonuclease activity to correct its mistake.

The kinetic studies are fully consistent with the results in wild-type *E. coli*. However, experiments carried out in double-knock-out cells that lack the genes responsible for expressing the MutY and Fpg repair proteins require additional discussion. MutY is the deoxyadenosine glycosylase that excises dA opposite OxodG and dG (*50*). Fapy·dG:dA base pairs are substrates for MutY in vitro, albeit poorer ones than OxodG:dA base pairs (*21*, *23*, *51*). Although Fapy·dG:dA base pairs are substrates for MutY, the frequency of G → T transversions are unaffected when cells lacking the gene for this protein (as well as that for Fpg) are transfected with M13 vectors containing Fapy·dG (Table 4). In contrast, OxodG-induced G → T transversions increased more than 7-fold in the *mutM/mutY* cells, indicating that OxodG:dA base pairs are repaired by MutY (and/or Fpg) in wild-type *E. coli*. We offer 3 hypotheses to explain the absence of an effect on Fapy·dG induced mutation frequencies when MutY is removed. The most obvious is that Fapy·dG:dA base pairs are not substrates for MutY in *E. coli*, even though the enzyme deglycosylates dA more rapidly opposite Fapy·dG than when it is part of a dG:dA base pair (*21*). It is also conceivable that because the mutation frequency of Fapy·dG borders on the detection limit of the REAP assay, that MutY may have a subtle effect on the levels of G → T transversions that is masked by the low signal-to-noise observed in these experiments. Alternatively, perhaps the low levels of Fapy·dG:dA base pairs produced in *E. coli* are below the radar of the cell's repair system. The plausibility of such a proposal is supported by studies on eukaryotic cells in which low doses of ionizing radiation failed to activate ATM-associated repair pathways (*52*).

Whether any of these hypotheses are correct does not change the most striking observation made in the course of the *E. coli* experiments, which is that the mutation frequency of Fapy·dG is significantly lower than in COS-7 cells. Replication of Fapy·dG containing vectors in simian kidney (COS-7) cells results in between 8.2% and 29.6% G → T transversions, depending upon the flanking sequence (*9*). Furthermore, the mutation frequencies from Fapy·dG replication were greater than those of OxodG. In vitro studies have shown that the eukaryotic bypass polymerase, pol η, exhibits increased infidelity when interacting with a carbocyclic model of Fapy·dG (*53*). However, the increased misincorporation frequency (<1%) for thymidine opposite the Fapy·dG model compound compared to when dG is in the template by pol η is not representative of the G → T mutations detected in the COS-7 cell or *E. coli* experiments. In addition, it is not known whether error prone polymerases are utilized in the mammalian cells when bypassing Fapy·dG. Our own experiments show that the analogous family of polymerases need not play a major role in the bypass of Fapy·dG in *E. coli*. Why Fapy·dG is so much more mutagenic in COS-7 cells than in *E. coli* is an unanswered question. However, the results described here clearly show that Fapy·dG is at most weakly mutagenic in wild-type *E. coli*.

SUPPORTING INFORMATION AVAILABLE

ESI-MS of synthetic oligonucleotides (4) containing Fapy·dG (**1a**−**d**) used to prepare the single stranded plasmids. This material is available free of charge via the Internet at http://pubs.acs.org.

REFERENCES

1. Neeley, W. L., and Essigmann, J. M. (2006) Mechanisms of Formation, Genotoxicity, and Mutation of Guanine Oxidation Products, *Chem. Res. Toxicol. 19*, 491−505.
2. Candeias, L. P., and Steenken, S. (2000) Reaction of HO• With Guanine Derivatives in Aqueous Solution: Formation of Two Different Redox-Active OH-Adduct Radicals and Their Unimolecular Transformation Reactions. Properties of G(-H)•, *Chem. Eur. J. 6*, 475−484.
3. Tan, X., Grollman, A. P., and Shibutani, S. (1999) Comparison of the Mutagenic Properties of 8-Oxo-7,8-dihydro-2′-deoxyadenosine and 8-Oxo-7−8-dihydro-2′-deoxyguanosine DNA Lesions in Mammalian Cells, *Carcinogenesis 20*, 2287−2292.
4. Le Page, F., Guy, A., Cadet, J., Sarasin, A., and Gentil, A. (1998) Repair and mutagenic potency of 8-oxoG:A and 8-oxoG:C base pairs in mammalian cells, *Nucleic Acids Res. 26*, 1276−1281.
5. Henderson, P. T., Delaney, J. C., Muller, J. G., Neeley, W. L., Tannenbaum, S. R., Burrows, C. J., and Essigmann, J. M. (2003) The Hydantoin Lesions Formed From Oxidation of 7,8-Dihydro-8-oxoguanine Are Potent Sources of Replication Errors in Vivo, *Biochemistry 42*, 9257−9262.
6. Henderson, P. T., Delaney, J. C., Gu, F., Tannenbaum, S. R., and Essigmann, J. M. (2002) Oxidation of 7,8-Dihydro-8-oxoguanine Affords Lesions That Are Potent Sources of Replication Errors in Vivo, *Biochemistry 41*, 914−921.
7. Wood, M. L., Esteve, A., Morningstar, M. L., Kuziemko, G. M., and Essigmann, J. M. (1992) Genetic Effects of Oxidative DNA Damage: Comparative Mutagenesis of 7,8-Dihydro-8-oxoguanine and 7,8-Dihydro-8-oxoadenine in *Escherichia coli*, *Nucleic Acids Res. 20*, 6023−6032.
8. Wang, D., Kreutzer, D. A., and Essigmann, J. M. (1998) Mutagenicity and Repair of Oxidative DNA Damage: Insights from Studies Using Defined Lesions, *Mutat. Res. 400*, 99−115.
9. Kalam, M. A., Haraguchi, K., Chandani, S., Loechler, E. L., Moriya, M., Greenberg, M. M., and Basu, A. K. (2006) Genetic Effects of Oxidative DNA Damages: Comparative Mutagenesis of the Imidazole Ring-Opened Formamidopyrimidines (Fapy Lesions) and 8-Oxo-purines in Simian Kidney Cells, *Nucleic Acids Res. 34*, 2305−2315.
10. Gajewski, E., Rao, G., Nackerdien, Z., and Dizdaroglu, M. (1990) Modification of DNA Bases in Mammalian Chromatin by Radiation-Generated Free Radicals, *Biochemistry 29*, 7876−7882.
11. Douki, T., Martini, R., Ravanat, J.-L., Turesky, R. J., and Cadet, J. (1997) Measurement of 2,6-Diamino-4-hydroxy-5-formamidopyrimidine and 8-Oxo-7,8-dihydroguanine in Isolated DNA Exposed to Gamma Radiation in Aqueous Solution, *Carcinogenesis 18*, 2385−2391.
12. Anson, R. M., Sentürker, S., Dizdaroglu, M., and Bohr, V. A. (1999) Measurement of oxidatively induced base lesions in liver from Wistar rats of different ages, *Free Rad. Biol. Med. 27*, 456−462.
13. Jaruga, P., Speina, E., Gackowski, D., Tudek, B., and Olinski, R. (2000) Endogenous Oxidative DNA Base Modifications Analysed With Repair Enzymes and GC/MS Technique, *Nucleic Acids Res. 28*, e16.

14. Hu, J., de Souza-Pinto, N. C., Haraguchi, K., Hogue, B. A., Jaruga, P., Greenberg, M. M., Dizdaroglu, M., and Bohr, V. A. (2005) Repair of Formamidopyrimidines in DNA Involves Different Glycosylases. Role of the OGG1, NTH1, and Neil 1 Enzymes, *J. Biol. Chem. 280*, 40544−40551.
15. Pouget, J.-P., Douki, T., Richard, M.-J., and Cadet, J. (2000) DNA Damage Induced in Cells by γ and UVA Radiation As Measured by HPLC/GC-MS and HPLC-EC and Comet Assay, *Chem. Res. Toxicol. 13*, 541−549.
16. Kamiya, H. (2003) Mutagenic Potentials of Damaged Nucleic Acids Produced by Reactive Oxygen/Nitrogen Species: Approaches Using Synthetic Oligonucleotides and Nucleotides, *Nucleic Acids Res. 31*, 517−531.
17. Cooke, M. S., Evans, M. D., Dizdaroglu, M., and Lunec, J. (2003) Oxidative DNA Damage: Mechanisms, Mutation, and Disease, *FASEB 17*, 1195−1214.
18. Wang, Y., Sheppard, T. L., Tomaletti, S., Maeda, L. S., and Hanawalt, P. C. (2006) Transcriptional Inhibition by an Oxidized Abasic Site in DNA, *Chem. Res. Toxicol. 19*, 234−241.
19. Cline, S. D., Riggins, J. N., Tornaletti, S., Marnett, L. J., and Hanawalt, P. C. (2004) Malondialdehyde Adducts in DNA Arrest Transcription by T7 RNA Polymerase and Mammalian RNA Polymerase II, *Proc. Natl. Acad. Sci. U.S.A. 101*, 7275−7280.
20. Greenberg, M. M. (2004) In Vitro and In Vivo Effects of Oxidative Damage to Deoxyguanosine, *Biochem. Soc. Trans. 32*, 46−50.
21. Wiederholt, C. J., Delaney, M. O., Pope, M. A., David, S. S., and Greenberg, M. M. (2003) Repair of DNA Containing Fapy·dG and Its β-C-Nucleoside Analogue by Formamidopyrimidine DNA Glycosylase and Mut Y, *Biochemistry 42*, 9755−9760.
22. Tchou, J., Bodepudi, V., Shibutani, S., Antoshechkin, I., Miller, J., Grollman, A. P., and Johnson, F. (1994) Substrate Specificity of Fpg Protein. Recognition and Cleavage of Oxidatively Damaged DNA, *J. Biol. Chem. 269*, 15318−15324.
23. Chmiel, N. H., Livingston, A. L., and David, S. S. (2003) Insight into the Functional Consequences of Inherited Variants of the hMYH Adenine Glycosylase Associated with Colorectal Cancer: Complementation Assays with hMYH Variants and Pre-steady-state Kinetics of the Corresponding Mutated E. coli Enzymes, *J. Mol. Biol 327*, 431−443.
24. Shibutani, S., Takeshita, M., and Grollman, A. P. (1991) Insertion of Specific Bases During DNA Synthesis Past the Oxidation-Damaged Base 8-OxodG, *Nature 349*, 431−434.
25. Lowe, L. G., and Guengerich, F. P. (1996) Steady-State and Pre-Steady-State Kinetic Analysis of dNTP Insertion Opposite 8-Oxo-7,8-dihydroguanine by *E. coli:* Polymerases I exo- and II exo-, *Biochemistry 35*, 9840−9849.
26. Wiederholt, C. J., and Greenberg, M. M. (2002) Fapy·dG Instructs Klenow Exo$^-$ to Misincorporate Deoxyadenosine, *J. Am. Chem. Soc. 124*, 7278−7279.
27. Pearson, C. G., Shikazono, N., Thacker, J., and O'Neill, P. (2004) Enhanced Mutagenic Potential of 8-Oxo-7,8-dihydroguanine When Present Within a Clustered DNA Damage Site, *Nucleic Acids Res. 32*, 263−270.
28. Delaney, S., Neeley, W. L., Delaney, J. C., and Essigmann, J. M. (2007) The Substrate Specificity of MutY for Hyperoxidized Guanine Lesions in Vivo, *Biochemistry 46*, 1448−1455.
29. Haraguchi, K., and Greenberg, M. M. (2001) Synthesis of Oligonucleotides Containing Fapy·dG (N6-(2-Deoxy-α,β-D-erythro-pento-furanosyl)-2,6-diamino-4-hydroxy-5-formamidopyrimidine), *J. Am. Chem. Soc. 123*, 8636−8637.
30. Haraguchi, K., Delaney, M. O., Wiederholt, C. J., Sambandam, A., Hantosi, Z., and Greenberg, M. M. (2002) Synthesis and Characterization of Oligodeoxynucleotides Containing Formamidopyrimidine Lesions and Nonhydrolyzable Analogues, *J. Am. Chem. Soc. 124*, 3263−3269.
31. Jiang, Y. L., Wiederholt, C. J., Patro, J. N., Haraguchi, K., and Greenberg, M. M. (2005) Synthesis of Oligonucleotides Containing Fapy·dG (N-(2-Deoxy-α,β-D-erythropentofuranosyl)-N-(2,6-diamino-4-hydroxy-5-formamidopyrimidine)) Using a 5′-Dimethoxytrityl Dinucleotide Phosphoramidite., *J. Org. Chem. 70*, 141−147.
32. Maniatis, T., Fritsch, E. F., and Sambrook, J. (1982) *Molecular Cloning*, Cold Spring Harbor Laboratory, Cold Spring Harbor, NY.
33. Creighton, S., Bloom, L. B., and Goodman, M. F. (1995) Gel Fidelity Assay Measuring Nucleotide Misinsertion, Exonucleolytic Proofreading, and Lesion Bypass Efficiencies, *Methods Enzymol. 262*, 232−256.
34. Creighton, S., and Goodman, M. F. (1995) Gel Kinetic Analysis of DNA Polymerase Fidelity in the Presence of Proofreading Using Bacteriophage T4 DNA Polymerase, *J. Biol. Chem. 270*, 4759−4774.
35. Delaney, J. C., and Essigmann, J. M. (1999) Context-Dependent Mutagenesis by DNA Lesions, *Chem. Biol. 6*, 743−753.
36. Delaney, J. C., and Essigmann, J. M. (2006) Assays for Determining Lesion Bypass Efficiency and Mutagenicity of Site-Specific DNA Lesions In Vivo, *Methods Enzymol. 408*, 1−15.
37. Kornyushyna, O., and Burrows, C. J. (2003) Effect of the Oxidized Guanosine Lesions Spiroiminodihydantoin and Guanidinohydantoin on Proofreading by *Escherichia coli* DNA Polymerase I (Klenow Fragment) in Different Sequence Contexts, *Biochemistry 42*, 13008−13018.
38. Smela, M. E., Hamm, M. L., Henderson, P. T., Harris, C. M., Harris, T. M., and Essigmann, J. M. (2002) The aflatoxin B1 formamidopyrimidine adduct plays a major role in causing the types of mutations observed in human hepatocellular carcinoma, *Proc. Nat. Acad. Sci. U.S.A. 99*, 6655−6660.
39. Brown, K. L., Deng, J. Z., Iyer, R. S., Iyer, L. G., Voehler, M. W., Stone, M. P., Harris, C. M., and Harris, T. M. (2006) Unraveling the Aflatoxin-Fapy Conundrum: Structural Basis for Differential Replicative Processing of Isomeric Forms of the Formamidopyrimidine-Type DNA Adduct of Afltoxin B1, *J. Am. Chem. Soc. 128*, 15188−15199.
40. Tudek, B., Graziewicz, M. A., Kazanova, O., Zastawny, T. H., Obtulowicz, T., and Laval, J. (1999) Mutagenic specificity of imidazole ring-opened 7-methypurines in M13mp18 phage DNA, *Acta Biochim. Pol. 46*, 785−799.
41. Asagoshi, K., Terato, H., Ohyama, Y., and Ide, H. (2002) Effects of a Guanine-Derived Formamidopyrimidine Lesion on DNA Replication, *J. Biol. Chem. 277*, 14589−14597.
42. Neeley, W. L., Delaney, J. C., Henderson, P. T., and Essigmann, J. M. (2004) In vivo Bypass Efficiencies and Mutational Signatures of the Guanine Oxidation Products 2-Aminoimidazolone and 5-Guanidino-4-nitroimidazole, *J. Biol.Chem. 279*, 43568−43573.
43. Kroeger, K. M., Goodman, M. F., and Greenberg, M. M. (2004) A Comprehensive Comparison of DNA Replication Past 2-Deoxyribose and its Tetrahydrofuran Analog in Escherichia coli, *Nucleic Acids Res. 32*, 5480−5485.
44. Greenberg, M. M., Hantosi, Z., Wiederholt, C. J., and Rithner, C. D. (2001) Studies on N4-(2-Deoxy-D-pentofuranosyl)-4,6-diamino-5-formamidopyrimidine (Fapy·dA) and N6-(2-Deoxy-D-pentofuranosyl)- 6-diamino-5-formamido-4-hydroxypyrimidine (Fapy·dG), *Biochemistry 40*, 15856−15861.
45. Burgdorf, L. T., and Carell, T. (2002) Synthesis, Stability, and Conformation of the Formamidopyrimidine G DNA Lesion, *Chem. Eur. J. 8*, 293−301.
46. Uesugi, S., and Ikehara, M. (1977) Carbon-13 Magnetic Resonance Spectra of 8-Substituted Purine Nucleosides. Characteristic Shifts for the Syn Conformation, *J. Am. Chem. Soc. 99*, 3250−3253.
47. Hamm, M. L., Rajguru, S., Downs, A. M., and Cholera, R. (2005) Base Pair Stability of 8-Chloro- and 8-Iodo-2′-deoxyguanosine Opposite 2′-Deoxycytidine: Implications Regarding the Bioactivity of 8-Oxo-2′-deoxyguanosine, *J. Am. Chem. Soc. 127*, 12220−12221.
48. Cheng, X., Kelso, C., Hornak, V., delos Santos, C., Grollman, A. P., and Simmerling, C. (2005) Dynamic Behavior of DNA Base Pairs Containing 8-Oxoguanine, *J. Am. Chem. Soc. 127*, 13906−13918.
49. Patro, J. N., Haraguchi, K., Delaney, M. O., and Greenberg, M. M. (2004) Probing the Configurations of Formamidopyrimidine Lesions Fapy.dA and Fapy.dG in DNA Using Endonuclease IV, *Biochemistry 43*, 13397−13403.
50. David, S. S., and Williams, S. D. (1998) Chemistry of Glycosylases and Endonucleases Involved in Base-Excision Repair, *Chem. Rev. 98*, 1221−1261.
51. Livingston, A. L., Kundu, S., Pozzi, M. H., Anderson, D. W., and David, S. S. (2005) Insight into the Roles of Tyrosine 82 and Glycine 253 in the *Escherichia coli* Adenine Glycosylase MutY, *Biochemistry 44*, 14179−14190.

52. Collis, S. J., Schwaninger, J. M., Ntambi, A. J., Keller, T. W., Nelson, W. G., Dillehay, L. E., and DeWeese, T. L. (2004) Evasion of Early Cellular Response Mechanisms following Low Level Radiation-induced DNA Damage, *J. Biol. Chem. 279*, 49624−49632.

53. Ober, M., Muller, H., Pieck, C., Gierlich, J., and Carell, T. (2005) Base Pairing and Replicative Processing of the Formamidopyrimidine-dG DNA Lesion, *J. Am. Chem. Soc. 127*, 18143−18149.

BI700628C